

Heat conduction in one-dimensional nonintegrable systems

Bambi Hu,^{1,2} Baowen Li,^{1,3,*} and Hong Zhao^{1,4}

¹*Department of Physics and Centre for Nonlinear Studies, Hong Kong Baptist University, Hong Kong, China*

²*Department of Physics, University of Houston, Houston Texas 77204-5506*

³*Department of Physics, National University of Singapore, 119260 Singapore*

⁴*Department of Physics, Lanzhou University, 730000 Lanzhou, China*

(Received 17 June 1999; revised manuscript received 24 November 1999)

Two classes of one-dimensional nonintegrable systems represented by the Fermi-Pasta-Ulam (FPU) model and the discrete ϕ^4 model are studied to seek a generic mechanism of energy transport on a microscopic level sustaining macroscopic behaviors. The results enable us to understand why the class represented by the ϕ^4 model has a normal thermal conductivity and the class represented by the FPU model does not even though the temperature gradient can be established.

PACS number(s): 44.10.+i, 05.45.-a, 05.70.Ln, 66.70.+f

Heat conduction in one-dimensional (1D) nonintegrable Hamiltonian systems is a vivid example for studying the microscopic origin of the macroscopic irreversibility in terms of deterministic chaos. It is one of the oldest but still a rather fundamental problem in nonequilibrium statistical mechanics [1]. Intended to understand the underlying mechanism of the Fourier heat conduction law, the study of heat conduction has attracted increasing attention in recent years [2–11].

Based on previous studies, we can classify the 1D lattices into three categories. The first one consists of integrable systems such as the harmonic chain. It was rigorously shown [12] that, in this category, no temperature gradient can be formed, and the thermal conductivity is divergent. The second category includes a number of nonintegrable systems such as the Lorentz gas model [2,10], the ding-a-ling and alike models [3], the Frenkel-Kontorova (FK) model [5], etc. In this category, the heat current is proportional to N^{-1} , and the temperature gradient $dT/dx \sim N^{-1}$; thus the thermal conductivity κ is a constant independent of system size N . The Fourier heat conduction law ($J = -\kappa dT/dx$) is justified. The third category also includes some nonintegrable systems such as the Fermi-Pasta-Ulam (FPU) [4,6] chain, the diatomic Toda chain [7], the (mass) disorder chain [8], the Heisenberg spin chain [9], and so on. In this category, although the temperature gradient can be set up with $dT/dx \sim N^{-1}$, the heat current is proportional to $N^{\alpha-1}$ with $\alpha \sim 0.43$, and the thermal conductivity $\kappa \sim N^\alpha$ is divergent as one goes to the thermodynamic limit $N \rightarrow \infty$.

These facts suggest that *nonintegrability is necessary to have a temperature gradient, but it is not sufficient to guarantee the normal thermal conductivity* in a 1D lattice. This picture prompts us to ask two questions of fundamental importance: (i) Why do some nonintegrable systems have normal thermal conductivity, while others fail? (ii) How can the temperature gradient be established in those nonintegrable systems having divergent thermal conductivities?

The reason for the divergent thermal conductivity in an integrable system is that the energy transports freely along

the chain without any loss, so that no temperature gradient can be established. The set up of temperature gradients in nonintegrable systems implies the existence of scattering. However, the different heat conduction behaviors in the two categories of nonintegrable systems indicate that the underlying mechanism must be different. To illustrate the point, let us write the Hamiltonian of a generic 1D lattice as

$$H = \sum_i H_i, \quad H_i = \frac{p_i^2}{2} + V(x_{i-1}, x_i) + U(x_i), \quad (1)$$

where $V(x_{i-1}, x_i)$ stands for the interaction potential of the nearest-neighbor particle, and $U(x_i)$ is an external (or on-site) potential. The origin of the external potential in real physical systems varies from model to model. For instance, in the FK model [5] the external potential is the interaction of the adsorbed atoms with the crystal surface. It is $U(x)$ that is distinguished from the two categories of nonintegrable lattices. $U(x)$ vanishes in all 1D lattices having divergent thermal conductivities. We are thus convinced that the *external potential plays a determinant role for normal thermal conduction*.

In this paper we would like to study the scattering mechanism and the role of the external potential in heat conduction in the two categories of nonintegrable systems. For this purpose, we choose two representatives from these two categories, i.e., the discrete ϕ^4 model (see, e.g. Ref. [13]) and the FPU model. Each model is the simplest anharmonic approximation of a monoatomic solid. In the ϕ^4 model, V takes a harmonic form, and the external potential $U(x) = mx^2/2 + \beta x^4/4$, with m fixed to be zero in this paper. In the FPU model, U vanishes and V takes an anharmonic form of $(x_i - x_{i-1})^2/2 + \beta(x_i - x_{i-1})^4/4$, and $\beta = 1$ throughout this paper. In the case of $\beta = 0$, the FPU model reduces to a harmonic chain.

In our numerical simulations the Nosé-Hoover thermostats [14] are put on the first and last particles, keeping them at temperatures T_+ and T_- , respectively. The motions of these two particles are governed by

$$\ddot{x}_1 = -\zeta_+ \dot{x}_1 + f_1 - f_2, \quad \dot{\zeta}_+ = \dot{x}_1^2/T_+ - 1,$$

*Author to whom correspondence should be addressed. Electronic address: bwli@phibm.hkbu.edu.hk

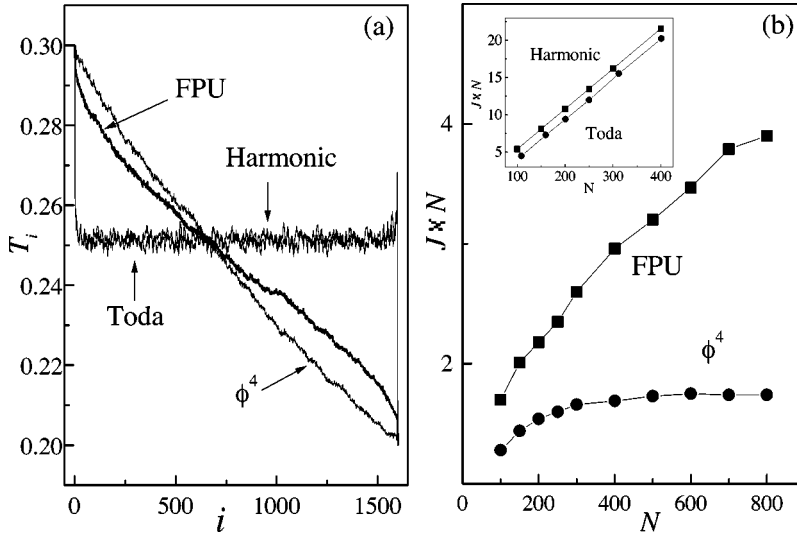


FIG. 1. (a) Temperature profiles for the FPU model, the ϕ^4 model, the harmonic and the monoatomic Toda model. (b) The quantity JN vs the system size N for the FPU model (solid square) and ϕ^4 (solid circle). Profiles of the harmonic and the monoatomic Toda are shown in the inset of (b). The lines in (b) and its inset are drawn to guide the eye. $T_+ = 0.3$, $T_- = 0.2$.

$$\ddot{x}_N = -\zeta_- \dot{x}_N + f_N - f_{N+1}, \quad \zeta_- = \dot{x}_1^2 / T_- - 1. \quad (2)$$

where $f_i = -(V' + U')$ is the force acting on the i th particle. The equation of motion of the other particle is $\ddot{x}_i = f_i - f_{i+1}$. The eighth-order Runge-Kutta algorithm was used. All computations are carried out to double precision. Usually the stationary state is set in after 10^7 time units. We should point out that we have performed computations using other types of thermostats, and no qualitative difference was found.

Figure 1(a) shows temperature profiles. In all nonintegrable systems, the temperature scales as $T = T(i/N)$. However, in the FPU case there is a singular behavior near the two ends, which is a typical character of 1D nonlinear lattices having divergent thermal conductivities. In the same figure we also show the temperature profiles for two integrable lattices: the harmonic and monoatomic Toda models. In these two cases no temperature gradient could be set up, and the stationary state corresponds to $T = (T_+ + T_-)/2$, which is consistent with the rigorous result [12].

In Fig. 1(b), we plot the quantity JN versus N for the FPU model and the ϕ^4 model. The inset shows the same quantity for the harmonic chain and the monoatomic Toda chain. The

local heat flux is defined by $J_i = \dot{x}_i (\partial V / \partial x_{i+1})$. We found that when the system reaches a stationary state, the time average $\langle J_i \rangle$ is site independent, and is denoted as J . For the harmonic chain and the monoatomic Toda chain JN is expected to be proportional to N since J is N independent. This is indeed the case, as illustrated in the inset. In both the FPU and ϕ^4 models dT/dx is proportional to $-1/N$, the thermal conductivity $\kappa = -J / (dT/dx) \propto JN$. Figure 1(b) shows that, in contrast to integrable systems and the FPU model, heat conduction in the ϕ^4 model obeys the Fourier law.

The heat current J in all nonintegrable systems decreases as the system size N is increased ($J \sim N^{\alpha-1}$, $0 < \alpha < 1$). To clarify the underlying mechanism we decompose the interaction of the thermostat into a series of kicks, and study the transport of a single kick along the chain. A free boundary condition is used in our calculation, but we should stress that the results do not depend on the type of boundary condition. In Fig. 2 we plot p_i versus i after a long time ($t = 800$) for four lattices: the harmonic chain (a), the monoatomic Toda chain (b), the FPU model (c), and the ϕ^4 model (d). The amplitude of the wave profile in the harmonic chain decreases continuously with time, but the global profile re-

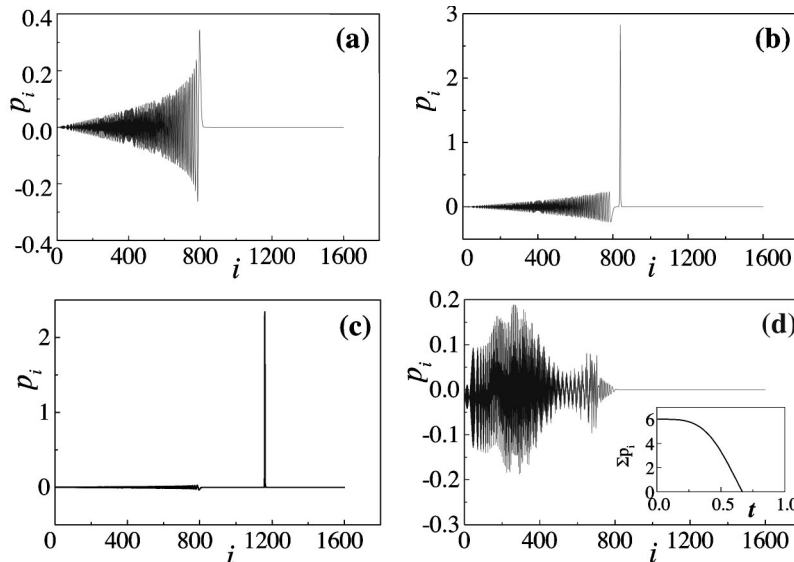


FIG. 2. The momentum excitation in different lattices. (a) The harmonic chain (b) The monoatomic Toda chain (c) The FPU model and (d) The ϕ^4 model. The inset in (d) illustrates the time evolution of the total momentum of the ϕ^4 chain.

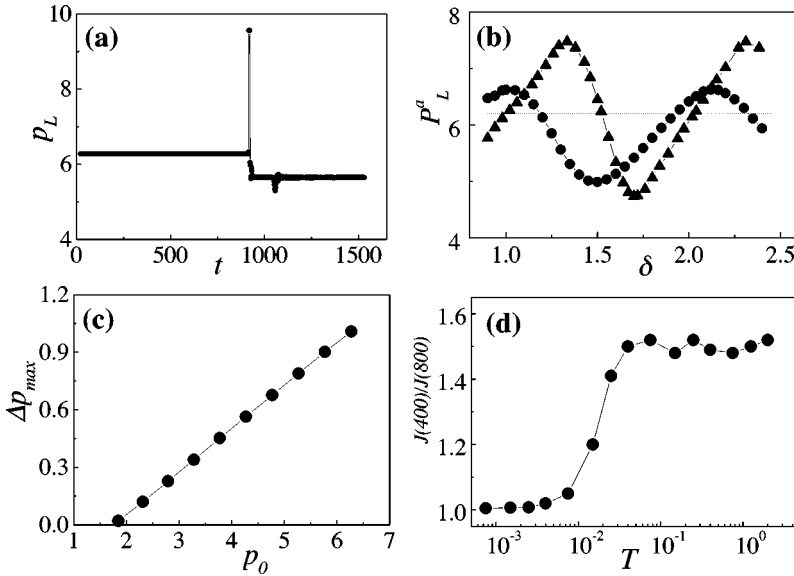


FIG. 3. (a) The time dependence of the momentum of a solitary wave. (b) The momentum (after collision) vs the phase. The solid triangle represents the results of the case in which both left and right solitary waves have the same initial momentum. The solid circle represents the case when solitary waves have different initial momenta (see the text for more in detail). The horizontal line is the momentum before collision. (c) The maximal momentum gain Δp_{max} vs initial momentum p_0 . (d) The ratio of the heat flux of $J(400)/J(800)$ vs the average temperature $T = (T_+ + T_-)/2$ on a semilogarithmic scale. The results shown here are for the FPU model.

mains unchanged. In both the FPU and Toda models, we observe that a solitary wave separates from the long tail. Initially this wave front is connected with other low amplitude excitations. After a certain time, this wave front moves faster, separates from the tail, and goes forward and retains its amplitude. In the meantime the tails behind it evolve in the same way as that in the harmonic chain. In the ϕ^4 model, the head part of the profile becomes weaker and weaker. The reason for this is that in the first three cases (a)–(c) both the total energy and the total momentum are conserved, whereas in the ϕ^4 model the momentum conservation breaks down due to the external potential. The inset in Fig. 2(d) shows that the total momentum in the ϕ^4 model decreases at least exponentially with time. The decay of the momentum with time indicates a loss of correlation. It is thus reasonable to envisage energy transport along the ϕ^4 chain as a random-walk-like scattering.

The solitary waves in the FPU chain exchange energy and momentum when colliding with each other. This causes energy loss, and the heat current decreases when the system size is increased. To show this, we begin two excitations at the two ends of the chain with different momenta; one moves to the right and the other to the left. Let $p_1 = 6$, $p_N = 3$, and $p_i = 0$ ($i \neq 1$ and N) be our initial excitations. We calculate the momenta of the solitary waves (by simply summing up momenta of several lattices around the peaks) and investigate the waves change before and after the interaction. We find that the larger wave generally transfers part of its momentum and energy to the smaller one, as shown in Fig. 3(a). The collision takes place at $t = 850$, where a peak is shown.

Moreover, the interaction between solitary waves is found to depend closely on a “phase” difference. Here the “phase” difference is defined as a time lag between the excitations of two solitary waves. For instance, if we excite a solitary wave from the left end at time t , and another one from the right end at time $t + \delta$, then δ is the “phase” difference. These two solitary waves, traveling through the chain in opposite directions, will collide with each other after a certain time. Although the physical meaning of the “phase” is not obvious, it is an important and good quantity to describe the interaction. We show p_L^a versus δ for two

different kinds of collision in Fig. 3(b), where p_L^a is the momentum of the solitary wave from the left after collision. In the first case both left and right solitary waves have the same initial momentum $p_L = p_R = 6.27$, which is excited by initial conditions of $p_1 = p_N = 6$ and $p_i = 0$ for other i . In the second case, the left wave has $p_L = 6.27$ and the right one $p_R = 3.28$, excited by initial conditions of $p_1 = 6$, $p_N = 3$, and $p_i = 0$ for $i \neq 1$ and N . The figure shows that P_L^a depends on the “phase” sinusoidally.

Other interesting features of the collision of solitary waves are shown in Fig. 3(c), where we plot the maximum momentum gain Δp_{max} versus the initial momentum p_0 for the FPU model. Δp_{max} is measured by subtracting the initial momentum p_0 from the maximum p_L in Fig. 3(b). First, this picture tells us that the exchange of momentum and energy depends on the initial momentum and energy. Second, there exists a critical momentum below which no energy exchange can take place. The critical $p_0^c \sim 1.8$ is clearly seen in the figure. For $p_0 < p_0^c$, Δp_{max} is zero. This result is very significant; it indicates that there exists a threshold for the solitary wave interaction, and below this threshold the interaction ceases, i.e., no momentum and energy is exchanged between the solitary waves. A direct consequence of this fact is the existence of a threshold temperature below which the FPU chain should behave like a harmonic chain; that is, the excited waves travel freely along the chain without any energy loss, no temperature gradient can be set up, and the heat current remains a constant even though the size of the chain is changed. To prove this argument, we show the quantity $J(400)/J(800)$ versus $T = (T_+ + T_-)/2$ in Fig. 3(d), where $J(N)$ is the heat current flux for a system of size N . In the case of a size-independent $J(N)$ one should obtain $J(400)/J(800) = 1$; otherwise one would obtain $J(400)/J(800) > 1$. Figure 3(d) captures this transition nicely for the FPU chain. The corresponding temperature threshold is about $T_c \sim 0.01$. In the region of $T \sim 0.001$ the numerical calculations do show that no temperature gradient is formed.

The different scattering mechanism in the FPU chain and those chains having normal thermal conductivities lead to a different temperature dependence of the thermal conductivity

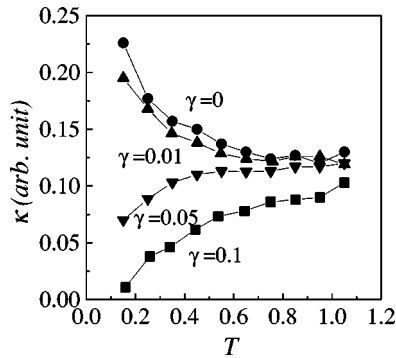


FIG. 4. The thermal conductivity $\kappa(T)$ for the FPU chain with an external potential $U(x) = -\gamma \cos(2\pi x)$.

$\kappa(T)$. In Fig. 4 we plot $\kappa(T)$ for a FPU chain with an external potential of form $U(x) = -\gamma \cos(2\pi x)$ for $\gamma=0, 0.01, 0.05$, and 0.1 . The chain size is fixed at $N=100$. As pointed out above, in a small γ regime such as $\gamma=0$ and 0.01 , the energy transport is assisted by the solitary waves, and the system has a large κ which decreases as the temperature is increased. However, in the opposite regime ($\gamma=0.05$ and 0.1), the energy transport is diffusive and obeys the Fourier law; κ increases with temperature, because more phonons are excited.

In summary, by studying two classes of 1D nonintegrable lattices, we have answered the two questions raised at the beginning: (i) The multiple scattering of the excited modes by the external potential leads to a decay (at least exponentially) of the correlation, so that a diffusive transport process can be reached, and the heat conduction obeys the Fourier law. (ii) Although the interaction of solitary waves makes it possible to set up a temperature gradient in the FPU and similar nonintegrable models, the momentum conservation prohibits the diffusive transport and consequently leads to a divergent thermal conductivity. In addition, we have uncovered an important fact in the FPU model, namely, the existence of a threshold temperature, below which the FPU mode behaves like a harmonic chain.

Note added in proof. After submission of this paper we became aware of the following results. Prosen and Campbell [15] proved in a more rigorous way that for a 1D classical many-body lattice total momentum conservation implies anomalous conductivity. The normal thermal conductivity in the ϕ^4 lattice has also been observed by Aoki and Kusnezov [16]. The role of the external potential has been further studied by Tsironis *et al.*, [17].

B.L. would like to thank G. Casati for useful discussions. This work was supported in part by the Hong Kong Research Grant Council and the Hong Kong Baptist University Faculty Research Grant program.

-
- [1] Chaos **8** (1998), focus issue on chaos and irreversibility; J. Lebowitz, *Physica A* **263**, 516 (1999); I. Prigogine, *ibid.* **263**, 528 (1999); D. Ruelle, *ibid.* **263**, 540 (1999).
- [2] J. L. Lebowitz and H. Spohn, *J. Stat. Phys.* **19**, 633 (1978).
- [3] G. Casati, J. Ford, F. Vivaldi, and W. M. Visscher, *Phys. Rev. Lett.* **52**, 1861 (1984); T. Prosen and M. Robnik, *J. Phys. A* **25**, 3449 (1992); D. J. R. Mimmagh and L.E. Ballentine, *Phys. Rev. E* **56**, 5332 (1997); H. A. Posch and Wm. G. Hoover, *ibid.* **58**, 4344 (1998).
- [4] H. Kaburaki and M. Machida, *Phys. Lett. A* **181**, 85 (1993); S. Lepri, R. Livi, and A. Politi, *Phys. Rev. Lett.* **78**, 1896 (1997).
- [5] B. Hu, B. Li, and H. Zhao, *Phys. Rev. E* **57**, 2992 (1998).
- [6] A. Fillipov, B. Hu, B. Li, and A. Zeltser, *J. Phys. A* **31**, 7719 (1998).
- [7] T. Hatano, *Phys. Rev. E* **59**, R1 (1999).
- [8] B. Hu, B. Li, and H. Zhao (unpublished).
- [9] A. Dhar and D. Dhar, *Phys. Rev. Lett.* **82**, 480 (1999).
- [10] D. Alonso, R. Artuso, G. Casati, and I. Guarneri, *Phys. Rev. Lett.* **82**, 1859 (1999).
- [11] P.-Q. Tong, B. Li, and B. Hu, *Phys. Rev. B* **59**, 8639 (1999).
- [12] Z. Rieder, J. L. Lebowitz, and E. Lieb, *J. Math. Phys.* **8**, 1073 (1967).
- [13] D. Chen, S. Aubry, and G. P. Tsironis, *Phys. Rev. Lett.* **77**, 4776 (1996).
- [14] S. Nosé, *J. Chem. Phys.* **81**, 511 (1984); W. G. Hoover, *Phys. Rev. A* **31**, 1695 (1985).
- [15] T. Prosen and D. K. Campbell, e-print [chao-dy/9908021](http://arxiv.org/abs/chao-dy/9908021).
- [16] K. Aoki and D. Kusnezov, e-print [chao-dyn/9910015](http://arxiv.org/abs/chao-dyn/9910015).
- [17] G. P. Tsironis, A. R. Bishop, A. V. Savin, and A. V. Zolotarev, *Phys. Rev. E* **60**, 6610 (1999).